Research Paper

# Chaos analysis of the cortical boundary for the recognition of psychosis

**Alexandra I. Korda, PhD; Christina Andreou, PhD; Mihai Avram, PhD; Marina Frisman; Mariya Aliqadri, MSc; Anita Riecher-Rössler, PhD; Heinz Handels, PhD; Thomas Martinetz, PhD; Stefan Borgwardt, MD**

**Background:** Structural MRI studies in people with first-episode psychosis (FEP) and those in the clinical high-risk (CHR) state have consistently shown volumetric abnormalities that depict changes in the structural complexity of the cortical boundary. The aim of the present study was to employ chaos analysis in the identification of people with psychosis based on the structural complexity of the cortical boundary and subcortical areas. **Methods:** We performed chaos analysis of the grey matter distribution on structural MRIs. First, the outer boundary points for each slice in the axial, coronal and sagittal view were calculated for grey matter maps. Next, the distance of each boundary point from the centre of mass in the grey matter was calculated and stored as spatial series, which was further analyzed by extracting the Largest Lyapunov Exponent (lambda [λ]), a feature depicting the structural complexity of the cortical boundary. **Results:** Structural MRIs were acquired from 77 FEP, 73 CHR and 44 healthy controls. We compared λ brain maps between groups, which resulted in statistically significant differences in all comparisons. By matching the λ values extracted in axial view with the Morlet wavelet, differences on the surface relief are observed between groups. **Limitations:** Parameters were selected after experimentation on the examined sample. Investigation of the effectiveness of the method in a larger data set is needed. **Conclusion:** The proposed framework using spatial series verifies diagnosis-relevant features and may contribute to the identification of structural biomarkers for psychosis.

## Introduction

Abnormalities in cortical surface areas and cortical thickness have been observed consistently in schizophrenia; these appear to be present during first-episode psychosis (FEP) and in the clinical high-risk state (CHR).[1] For instance, Drobinin and colleagues[2] reported that youth with psychotic symptoms showed an overall trend toward lower cortical folding across all brain regions. Wisco and colleagues[3] reported reduced metric distortion in patients with schizophrenia compared with demographically matched healthy controls in the left inferior frontal gyrus, more specifically in the Broca area. Haatveit and colleagues[4] found negative associations between brain volume, thickness, surface area and cognition in the left anterior cingulate cortex in patients with schizophrenia, which may point to abnormal neurodevelopment. Madre and colleagues[5] showed reduced gyrification index in patients with schizophrenia. Since this metric is associated with the geometry and curvature of the brain's cortical surface, their results suggest that patients with schizophrenia are influenced by additional neurodevelopmental and genetic factors. Environmental and neurodegenerative factors have been indicated to regulate cortical thickness, while surface areas may be predominantly influenced by early neurodevelopmental and genetic factors.[6,7] Therefore, features that characterize structural surface irregularities of the brain might reveal information about the pathogenesis of schizophrenia that is somewhat independent of the duration or onset of illness[8] and may be helpful in the individualized detection of psychosis risk.

We performed chaos analysis of the grey matter distribution on structural MRIs from CHR individuals without later transition to psychosis, CHR individuals with later transition, FEP patients and healthy controls. By transforming MRI grey matter maps into spatial series, we aimed to compare the structural complexity of the cortical boundary across the 4 groups. A spatial series is the distribution of the distance of the boundary points in the surface from the centre of the mass in grey matter images. The conversion of images into sequences for applications of time-series analysis tools has been used for solving several problems in image data mining.[9] As grey matter morphology is inherently complex,

**Correspondence to:** A. Korda, Ratzeburger Allee 160, 23538 Lübeck, Germany; alexandra.korda@uksh.de

Submitted Sep. 1, 2022; Revised Feb. 20, 2023; Accepted Feb. 20, 2023

**Cite as:** *J Psychiatry Neurosci* 2023 April 25;48(2). doi: 10.1503/jpn.220160

chaos and nonlinear dynamics analyses are suitable mathematical techniques for extracting informative statistical properties.[10] A previous study reported differences in the complexity of brain folding in Alzheimer disease and aging[11,12] by transforming MRI scans into spatial series and comparing the Largest Lyapunov Exponent (lambda [λ]) values between patients and controls.

In this study, we explore the λ to determine the chaotic behaviour and nonlinear dynamics from spatial-series data of grey matter distribution in early psychosis. Here, λ is tackled as a geometric shape descriptor of cortical surface morphology that considers subcortical areas, in addition to its surface.[10] It expresses the divergence of the small distances over the cortical boundary, and thus can be used as a quantitative measure of geometry and curvature, and therefore morphological complexity of the cortical surface. The aim of the present study was to analyze the chaotic dynamic of the grey matter cortical surfaces in the early stages of psychosis, and its usefulness for marking the progression of the illness. We show that this approach provides interesting insights for distinguishing both FEP and CHR individuals from healthy controls at the group level and goes beyond that of standard volumetric comparisons using voxel-based morphometry (VBM). To this end, we investigated hidden patterns in the grey matter cortical surface areas and subcortical areas on group and single-subject levels. We hypothesized that the nonlinear dynamics of brain folding in FEP and CHR would differ from that of healthy controls. We performed a group-level analysis providing insights on the differentiation of both groups from healthy controls regarding the structural complexity of their cortical boundary. Additionally, we performed a single-subject level analysis that led to recognition of FEP based on the surface relief using the wavelet transformation on the λ values.

## Methods

### *Study participants*

The current analyses are based on data from patients included in the early detection of psychosis project (FePsy) at the Department of Psychiatry of the University of Basel[13] between November 2008 and April 2014 (61 CHR individuals without later transition to psychosis and 12 with later transition, 77 FEP patients, and 44 healthy controls). FePsy was a prospective clinical study of all consecutive referrals to the specialized early detection centre of the 2 cantons Basel–Stadt and Basel–Landschaft (FePsy). The CHR participants were followed up until transition (CHR-T), or if no transition occurred (CHR-NT) for a maximum of 5 years. For screening purposes, the Basel Screening Instrument for Psychosis (BSIP) was used, a 46-item instrument based on variables that are risk factors or early symptoms of psychosis, such as prodromal symptoms, social decline, drug abuse, previous psychiatric disorders or genetic liability for psychosis.[14] Clinical high-risk status was defined based on either relief of psychotic symptoms; short-term, intermittent psychotic symptoms; or a first- or second-degree relative with a psychotic disorder and at least 2 psychotic risk factors. First-episode psychosis status and transition to psychosis were assessed using the criteria of Yung and colleagues[15]: a score of 4 or higher on the Brief Psychiatric Rating Scale (BPRS) item hallucinations or a score of 5 on the BPRS item bizarre thought content, disbelief or conceptual disturbance had to be included. Symptoms must have lasted for at least 1 week and must have occurred several times a week. A patient with FEP is one who already meets the criteria for transition to psychosis, as defined by Yung and colleagues.[15] Their criteria for defining psychosis represent boundaries across the staging continuum and do not necessarily imply that these patients have progressed from the CHR status. The CHR-T individuals were those classified as CHR at baseline (i.e., they had never reached the psychosis cutoff, according to the criteria of Yung and colleagues) who progressed to psychosis during follow-up. The MRIs were therefore recorded at different stages of the psychosis continuum for CHR-T (before transition) and FEP (after the onset of overt psychosis).

All participants who had MRIs available at baseline were included in the study. Exclusion criteria were age younger than 18 years; lack of knowledge of German; IQ lower than 70; previous psychotic episode treated with antipsychotics for more than 3 weeks; and diagnosed brain disorder, substance dependence (other than cannabis dependence), secondary psychotic symptoms within a single depressive episode, bipolar disorder or borderline personality disorder. Patients were taking low-dose atypical antipsychotics for behaviour management and were referred to FePsy by a psychiatrist or general practitioner. Healthy controls were recruited from the same region as the CHR group through local advertising and were group-matched for age, gender, handedness and education level. These individuals, as assessed by an experienced psychiatrist, had no current psychiatric disorders, head trauma, neurologic disorders, major medical or surgical ailments, or substance dependence (other than cannabis and nicotine), and there was no family history of mental illness as determined in a detailed clinical interview. The study was approved by the local ethics committee of the University of Basel, and written informed consent was obtained from each participant. The study was conducted in accordance with the Declaration of Helsinki. Data were only to be made available via a request to the authors, 2 of whom are authors of the present study (A.R.-R. and S.B.).

Participants were scanned using a Siemens MAGNETOM Vision 1.5 T scanner at the University Hospital, Basel. A 3-D volumetric spoiled gradient recalled echo sequence generated 176 contiguous, 1-mm-thick sagittal slices. Imaging parameters were echo time 4 ms, repetition time 9.7 ms, flip angle 12°, matrix size 200 × 256, field of view 25.6 × 25.6 cm, voxel dimensions 1.28 × 1 × 1 mm. Inclusion and exclusion criteria were described in a previous study.[1]

### *MRI data preprocessing*

After inspection for artifacts and gross abnormalities, the MRI scans were segmented into grey matter, white matter and cerebrospinal fluid (CSF) tissue maps in native space using

the CAT12 toolbox (http://dbm.neuro.uni-jena.de), an extension of the SPM12 software package (Wellcome Department of Cognitive Neurology). Specifically, the CAT12 toolbox extends the integrated segmentation model, which consists of MRI field intensity nonuniformity correction, spatial normalization and tissue segmentation, with several preprocessing steps to further improve the quality of data. Initially, Coupe and colleagues[16] applied the method described by Wiest-Daesslé and colleagues[17] to MRI scans to increase the signal-to-noise ratio of the data. The usual streak artifacts in modulated images are greatly reduced by the default internal interpolation setting "Fixed 1 mm" in the CAT12 toolbox. The MRI scans were subsequently separated into grey matter, white matter and CSF tissues using an adaptive maximal posterior segmentation approach[18] augmented with partial volume estimation.[19] The segmentation step was completed by applying spatial constraints to the segmented tissue probability map based on a hidden Markov random field model[20] that removes isolated voxels and gaps that are unlikely to belong to a particular tissue class, resulting in a higher signal-to-noise ratio of the final tissue probability maps. Filter strength was automatically determined by estimating the residual noise in the image. The original voxels were projected to new positions in the warped image while preserving the specific tissue volume within the voxels (i.e., generated by affine transformation [global scaling] and nonlinear warping [local volume modification]). Then, for each participant, modulated warped grey matter images (mwp1*) with an isotropic voxel size of 1.5 mm were selected for spatial series extraction. All scans were reviewed by a neuroradiologist to rule out clinically significant abnormalities. Then the mwp1* image was selected for the extraction of the spatial series.

For each MRI slice, a corresponding spatial series was obtained by measuring the distances clockwise from outer boundary points to the grey matter centre of mass, as described by Chen and colleagues,[11] using the function centre of mass in MATLAB 2020b. A graphical representation of the centre of mass of 1 participant is presented in Appendix 1, Figure S1, available at jpn.ca/lookup/doi/10.1503/jpn.220160/tab-related-content. By computing the distances between the boundary points and the grey matter centre of each axial, coronal and sagittal view slice, these spatial series can capture the morphology of the cortical surface, including its folding patterns and shape changes. Figure 1A shows

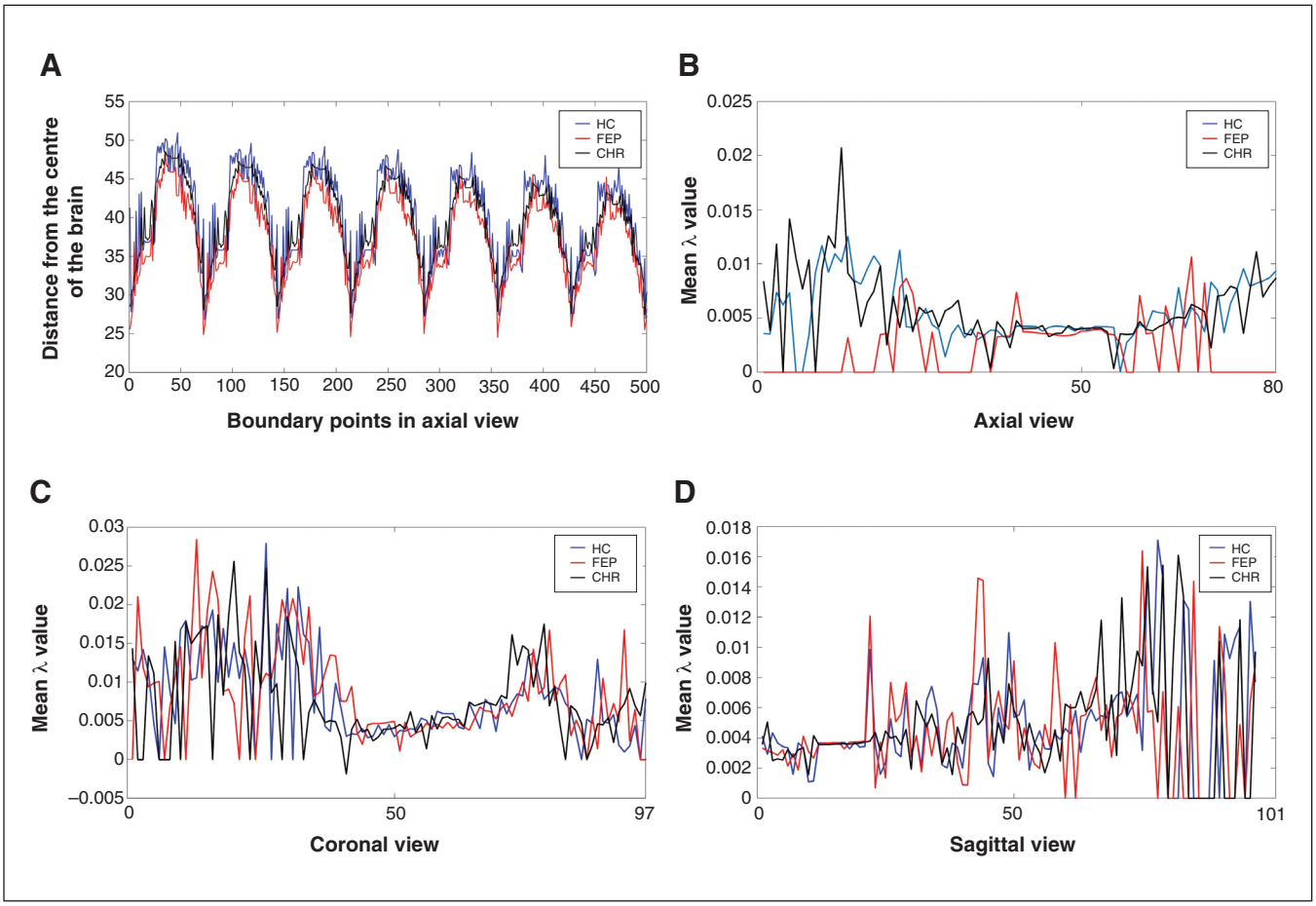


**Fig. 1:** Distance from the centre of the brain and the outer boundary extracted from 3 participants — 1 healthy control (HC), 1 participant with first-episode psychosis (FEP) and 1 participant in a clinical high-risk (CHR) state — in the (A) axial view. The mean λ values in the (B) axial view, (C) coronal view and (D) sagittal view are shown.

examples of the corresponding generated spatial series of 1 CHR, 1 FEP and 1 healthy control participant. The spatial series alone is not an adequate measure for the discrimination of the groups, while the λ values in Figure 1B–D show a differentiation among groups, which is validated with statistical analysis. In all views, the same slices were selected from all participants. From the axial view 81 slices were selected, from the coronal view 97 slices, and from the sagittal view 101 slices. The length of the spatial series extracted varied for each view.

*Largest Lyapunov Exponent and wavelet transformation*

The numerical technique for the calculation of the λ and the wavelet transformation is presented in Appendix 1 and has been used in previous studies.[21,22] The mean of the λ values was calculated for each slice, concluding in 81 values per participant in axial view, 97 values in coronal view and 101 values in sagittal view. Figure 1 shows examples of the extracted distances in axial view, and the mean value of the corresponding generated λ values of 1 CHR, 1 FEP and 1 healthy control participant. The mean value of λ diverges across slices in the 3 groups, depicting the structural abnormalities of the cortical boundary (Figure 1B–D).

A wavelet transformation allowed visualization of the structural roughness of the spatial λ series.[22] At each boundary point and for each scale (inverse frequency), a value was obtained for the match of the Morlet wavelet (Appendix 1, Figure S2) with the λ series. As the scales are inverse frequencies, the larger the scale the smaller the frequency in the λ signal. Small frequencies in the λ signal represent low cortical complexity. The correlation between these signals is presented as an image, called a scalogram. Such scalograms can be used to better understand the dynamic behaviour of a system and can also be used to distinguish signals produced by different systems. The different scales depict the level of the structural complexity on the cortical boundary.

Additionally, surface-based morphometry analysis was implemented to calculate the gyrification index using the CAT12 toolbox. General linear models for group comparisons were applied. We calculated the gyrification index based on absolute mean curvature,[23] using a 20 mm kernel, as suggested in the CAT12 manual, for folding data.

## Results

*Sociodemographic characteristics*

There were no significant differences between the FEP and control groups with respect to age and alcohol consumption. For the comparison between the FEP and CHR groups, there were no significant differences with respect to age, years of education, smoking, alcohol consumption and gender. There were significant differences between the FEP and CHR groups with respect to total and positive symptoms assessed with the BPRS and negative symptoms assessed with the BPRS and the Scale of Negative Symptoms (SANS), and there were significant differences between the CHR and control groups with respect to sex (Appendix 1, Table 1).

*Statistical results and localization*

Student *t* tests were conducted with the significance level set at $p < 0.05$ for the distance values and the mean λ values of the following group comparisons: FEP v. controls, FEP v. CHR-NT, FEP v. CHR-T, CHR-NT v. controls and CHR-T v. controls. There were no statistically significant differences between groups for the distance values. For the comparison between the FEP and control groups, the mean λ values from all slices in the axial view differed significantly (false discovery rate [FDR]–corrected $p < 0.05$), while there were no significant differences in the mean λ values in the coronal and sagittal views. In addition, the comparisons of the mean λ values between the FEP and CHR-NT groups and between the FEP and CHR-T groups also showed differences only in the axial view. Hence, it can be concluded that mean λ values of the axial view might suffice for detecting differences between FEP and comparison groups.

The slices that had significant FDR-corrected *p* values for the comparisons between the CHR-NT and control groups and between the CHR-T and control groups in axial and sagittal views were selected and mapped on the brain using the aal.nii map in the MRIcron toolbox. The mean λ values in the CHR-NT group differed significantly from those in the control group in the 85th slice in the axial view (with the initial reference point set at the 15th slice measuring from the cerebellum), which contains many regions such as the thalamus, cingulum, cuneus and caudate, and in the 21st, 22nd, 24th and 27th slices in sagittal view, which contain the cerebellum, fusiform and right inferior temporal gyrus (Figure 2A). The mean λ values in the CHR-T group differed significantly from those in the control group with the initial reference point set at the 29th slice starting from the cerebellum in the sagittal view, which contains the cerebellum, part of the vermis, the fusiform gyrus, the temporal pole of the middle temporal gyrus and the inferior temporal gyrus (Figure 2B). The greatest mean λ value is presented for the control group, depicting the high complexity of the cortical surface for a healthy brain.

For comparison, VBM analyses were performed in the SPM12 toolbox on mwp1* images to identify volumetric brain differences for the following group comparisons: FEP v. controls, CHR v. controls and FEP v. CHR. The demographic variables education (yr), years of smoking (cigarettes per day), alcohol, age and sex were used as covariates. The BPRS total, BPRS positive, BPRS negative, Global Assessment of Functioning (GAF) and SANS scores were used as additional covariates in the comparison between the FEP and CHR groups. There were no significant differences for family-wise error (FWE)–corrected *p* values in all 3 group comparisons.

As mentioned, the mean λ values in the FEP group differed significantly from those in both the control and CHR groups in the axial view for all slices. For this reason, we further analyzed the λ values extracted from all axial view slices using the wavelet transformation to assess whether a spatial-scale representation might make visualization of group differences possible. The λ values from each slice were stacked horizontally, resulting in a vector of 39 334 points for each

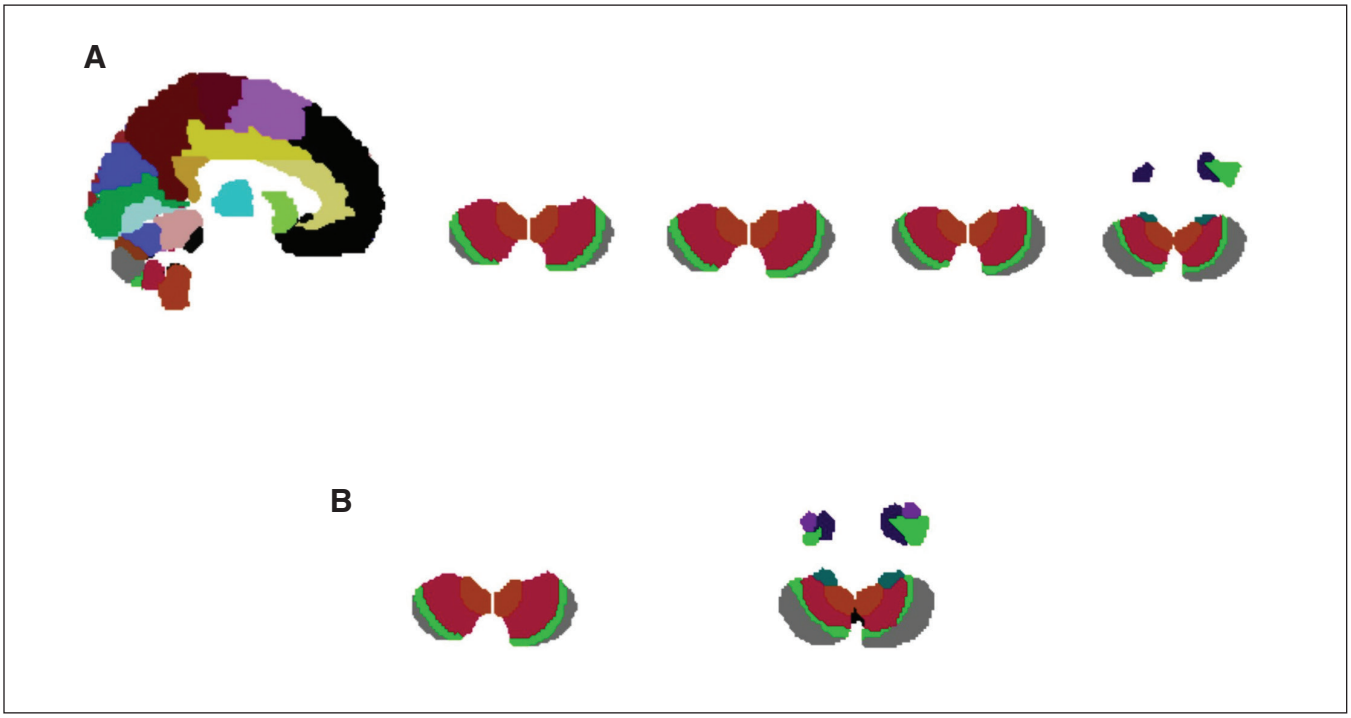


**Fig. 2:** Slices that had significant false discovery rate–corrected *p* values for (A) the comparison between the clinical high-risk group with no transition to psychosis (CHR-NT) and healthy controls in the 85th slice in the axial view and the 21st, 22nd, 24th and 27th slices in the sagittal view and (B) the comparison between the CHR group with transition to psychosis (CHR-T) and healthy controls in the 22nd and 29th slices in the sagittal view.

participant (number of slices in each view × number of the boundary points). A zoom representation of these series is shown for 1 participant from each group in Figure 1. In the present study, we used 20 wavelet scales (inverse frequency), which were selected after experimentation. Larger scales did not contain further information for the CHR and control groups. Figure 3 shows example scalograms of 1 FEP, 1 CHR and 1 control participant. The 77 FEP patients presented a common pattern like that shown in Figure 3A, with a higher correlation with the Morlet wavelet in large scales for the 15th to 30th slices in the axial view. The initial reference point was set at the 15th slice measuring from the cerebellum (Appendix 1, Figure S3 and S4).

Student *t* tests for each scale were conducted for group comparisons, with significance set at $p < 0.05$. The FDR-corrected *p* values for the comparisons between the FEP and control groups and between the FEP and CHR groups are shown in Figure 4. The FEP group differed significantly from both the control and CHR groups in all scales in the axial view. However, there were no significant differences in gyrification index in all comparisons (FDR-corrected $p < 0.05$).

## Discussion

In the present study, we investigated grey matter abnormalities in the spatial-scale domain for a large sample of participants with FEP and CHR as well as healthy controls. The methods applied in this study are well established in the image and signal analysis. The method of Largest Lyapunov Exponent expresses the way that 2 distance neighbour points in the phase space diverge across the surface with respect to all the other distance points in the boundary, and the correlation with the Morlet wavelet in different scales depicts the surface relief. Therefore, λ allows identification of grey matter abnormalities, and wavelet transformation allows visual inspection of the level of the structural complexity of the cortical boundary. Under this assumption and using the mean λ value from each slice in the axial view, we observed a specific pattern that differentiated the FEP group from all other groups, even from the CHR-T group.

Our method needs to be refined in further studies. The slices from the 15th to 95th in the axial view, 25th to 125th in the coronal view and 7th to 103rd in the sagittal view as well as the initial reference point set starting from the cerebellum were selected after experimentation to be able to identify a total boundary of the grey matter image. The λ values calculated on the first 15 slices in the axial view in the FEP group (with the first slice starting from the cerebellum set as the initial reference point) present a specific pattern that differentiates the FEP group from all other groups based on a simple visual inspection of the scalograms (Appendix 1, Figures S3 and S4). Taking into account that the divergence of the distances may be affected by subcortical structures, distinct patterns for FEP were located on the right and left cerebellum, vermix, bilateral temporal poles, and left central and prefrontal regions. The high correlation of the FEP λ series with

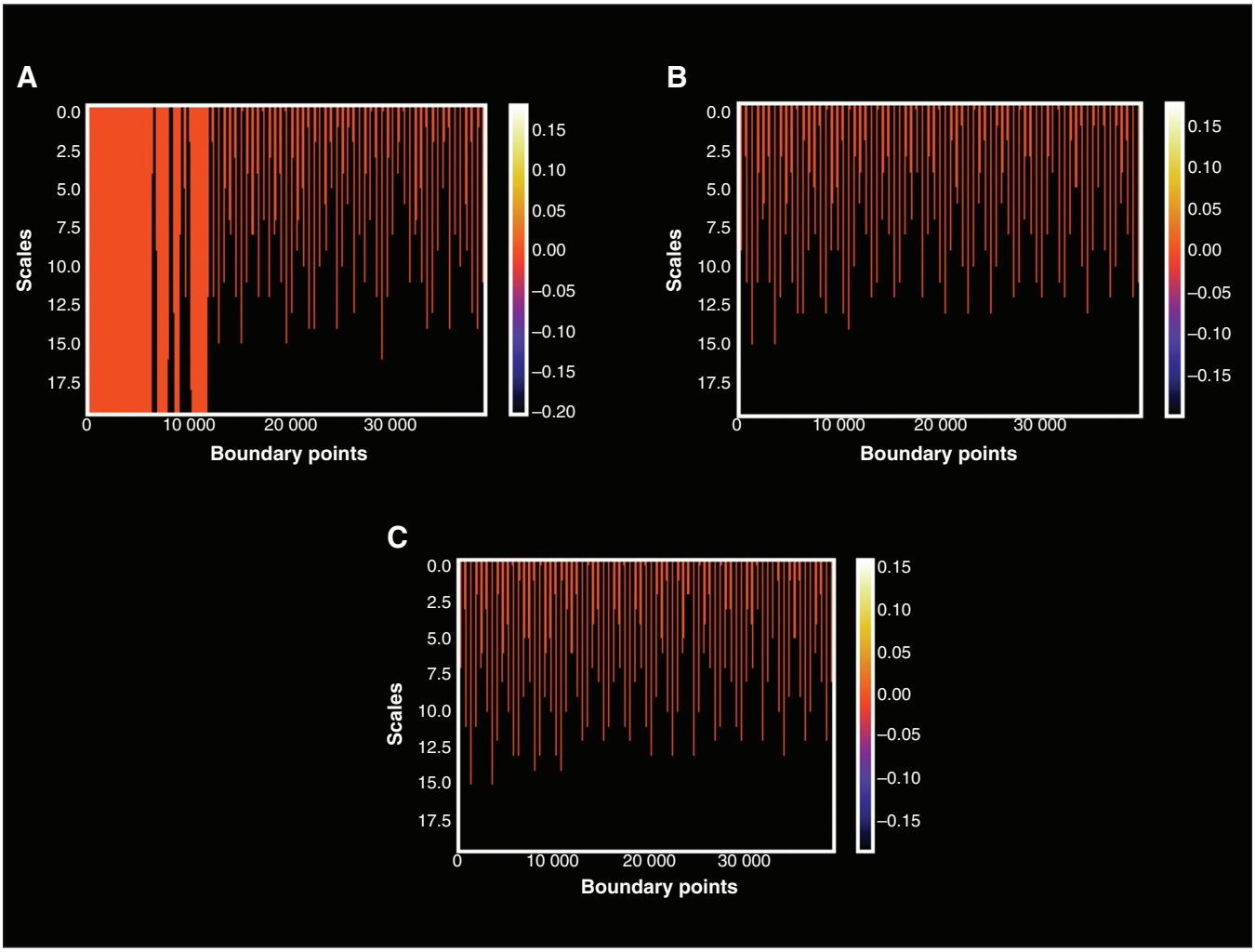


**Fig. 3:** Scalogram of (A) 1 participant with first-episode psychosis, (B) 1 participant in the clinical high-risk state and (C) 1 healthy control participant.

the Morlet wavelet observed in every slice of axial view for high scales depicts low cortical complexity for FEP. Thus, the significant differences observed between the FEP group and the other groups reflect the low structural complexity of the cortical boundary captured in the axial view for the FEP group. As the scales depict the inverse frequencies, which represent the surface relief, the λ series extracted from the FEP group reflects a smoother divergence of the distances across the cortical boundary compared with the control and CHR groups, which may reflect a gyrification decrease for the FEP group in the above-mentioned regions. These results are consistent with those of previous studies that showed a significant reduction in cortical folding across multiple brain regions, especially the left frontal and right temporal regions, in patients with FEP compared with healthy controls.[24–26]

Abnormal brain morphology has also been observed in CHR individuals,[27] while gyrification network measures can predict later transition to psychosis.[28] These observations are in line with our findings that cortical folding differed between both the CHR-NT and CHR-T groups and the control group in various regions. Previous studies have shown gyrification differences between both CHR-NT and CHR-T groups and healthy controls in the left medial occipital regions[27,29] as well as volumetric differences in the right temporal lobe and middle temporal lobe.[30,31] The later regions were also identified as potential biomarkers for CHR with later transition in this study. Regions included in the above-mentioned slices may be considered for further investigation in a region of interest analysis.

The innovation of the proposed method is that it uses spatial series extracted from structural MRI, which separates it from many other studies investigating grey matter volume increase or decrease, as is the case with, for example, VBM analyses. Instead, our approach transforms the brain MRI into a spatial series from each slice and calculates the dynamics of the grey matter distribution in each slice using λ. To the best of our knowledge, this is the first use of λ for the comparison of the cortical boundary complexity in FEP and CHR participants. In the examined data set, there were no significant differences in gyrification index in the surface-based morphometry analysis.

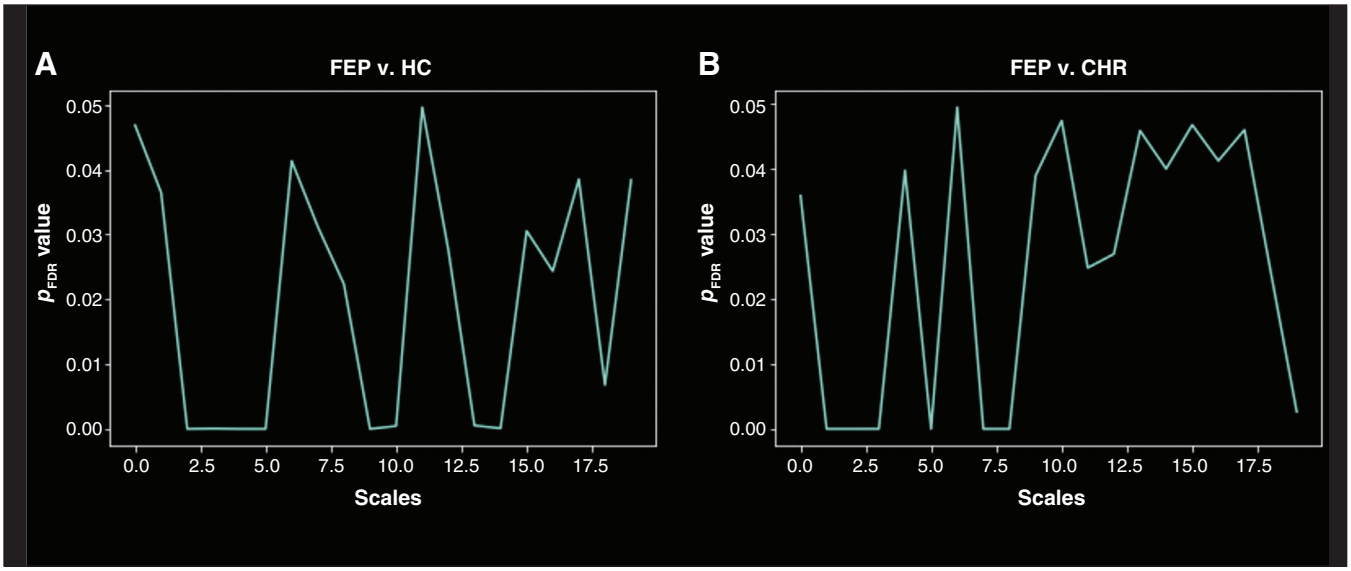


**Fig. 4:** Significant differences in scales (false-discovery rate [FDR]–corrected $p < 0.05$) for the comparisons between (A) the first-episode psychosis (FEP) and healthy control (HC) groups and (B) the FEP and clinical high-risk (CHR) state groups.

Thus, we conclude that the changes in brain morphology represented by chaos analysis provide better insights for recognition of psychosis than static alteration measures in brains of patients with psychotic disorders. The λ values calculated on the cortical boundary can be a new way to measure the subtle cerebral reorganization changes in psychotic disorders,[32,33] especially when the cortical surface complexity is combined with the complexity in brain topology.[21] Thickness also indirectly influences boundary complexity and relates both measures. The λ values calculated in the cortical folding can be considered a combination of cortical features, such as cortical thickness, folded area, cortical gyrification and sulcal depth, into an integrated index, in a similar way as fractal dimension in a study by Im and colleagues.[34] Previous longitudinal studies have shown prognostic associations with gyrification index.[35] Future studies that apply the proposed method in a larger data set are warranted to investigate the association between λ values extracted from the cortical surface and subcortical regions, core clinical symptoms and duration of untreated illness at baseline.

The main advantage of the proposed method is that we can calculate the λ for each participant without regard for their head size, as differences in brain volume do not affect the values of λ.[10] In addition, λ is not affected by the initial point of reference; i.e., the centre of mass in participants' grey matter images, which is used for the calculation of the distance to boundary points. As λ expresses the way in which 2 neighbour points in the state space diverge across the surface with respect to all the other points in the boundary, we may consider it for identification of grey matter abnormalities in specific cortical and subcortical structures. It should be noted that scalograms (showing visible differences between FEP, control and CHR groups) were available approximately 1 hour after the MRI scan by using a PC with Intel Core i7 processors 10th generation, thus making our method very attractive for biomarker research.

The method seems promising, as it allows for recognition of psychosis based on the structural complexity of the cortical boundary and reveals how the cortex is folded in the progression of psychosis. Thus, investigating the complexity of the cortical boundary might lead to the identification of more specific imaging biomarkers that may provide greater insight into the neurobiology of psychiatric disorders.

### *Limitations*

Our study had some limitations. The method contains many parameter selections, the effects of which should be investigated. The sample size was moderate; moreover, different scanning parameters across different (including non-psychotic) diagnoses have to be investigated for the effectiveness and robustness of the method.

## Conclusion

Our results can be used to refine prognostic and etiopathological research on early psychosis and the progression of illness. Longitudinal studies are needed to investigate the implications of these findings for the development of psychotic illnesses. Further studies in large cohorts will identify key regions and key structural features that characterize psychotic disorders, improve our understanding of the neurobiological changes that occur before the onset of psychosis, and provide ways to prevent and treat CHR.

**Affiliations:** From the Department of Psychiatry and Psychotherapy, Translational Psychiatry, University of Luebeck, Germany (Korda, Andreou, Avram, Frisman, Borgwardt); the Department of Applied Natural Sciences, Biomedical Engineering, Technical University of Luebeck (Aliqadri); the Medical Faculty, University of Basel, Switzerland (Riecher-Rössler); the Institute of Medical Informatics, University of Luebeck, Germany (Handels); the Institute for Neuro- and Bioinformatics, University of Luebeck, Germany (Martinetz).

**Competing interests:** None declared.



## References


1. Borgwardt S, Koutsouleris N, Aston J, et al. Distinguishing prodromal from first-episode psychosis using neuroanatomical single-subject pattern recognition. *Schizophr Bull* 2013;39:1105-14.
2. Drobinin V, Van Gestel H, Zwicker A, et al. Psychotic symptoms are associated with lower cortical folding in youth at risk for mental illness. *J Psychiatry Neurosci* 2020;45:125-33.
3. Wisco JJ, Kuperberg G, Manoach D, et al. Abnormal cortical folding patterns within Broca's area in schizophrenia: evidence from structural MRI. *Schizophr Res* 2007;94:317-27.
4. Haatveit B, Mørch-Johnsen L, Alnæs D, et al. Divergent relationship between brain structure and cognitive functioning in patients with prominent negative symptomatology. *Psychiatry Res Neuroimaging* 2021;307:111233.
5. Madre M, Canales-Rodríguez EJ, Fuentes-Claramonte P, et al. Structural abnormality in schizophrenia versus bipolar disorder: a whole brain cortical thickness, surface area, volume and gyrification analyses. *Neuroimage Clin* 2020;25:102131.
6. Rimol LM, Nesvåg R, Hagler DJ, et al. Cortical volume, surface area, and thickness in schizophrenia and bipolar disorder. *Biol Psychiatry* 2012;71:552-60.
7. Birnbaum R, Weinberger DR. Genetic insights into the neurodevelopmental origins of schizophrenia. *Nat Rev Neurosci* 2017;18:727-40.
8. Zhao C, Zhu J, Liu X, et al. Structural and functional brain abnormalities in schizophrenia: a cross-sectional study at different stages of the disease. *Prog Neuropsychopharmacol Biol Psychiatry* 2018;83:27-32.
9. Réjichi S, Chaabane F. Brain tumor extraction using graph based classification of MRI time series for diagnostic assistance. *2016 International Symposium on Signal, Image, Video and Communications (ISIVC)* 2016:320-4.
10. Zhao G, Denisova K, Sehatpour P, et al. Fractal dimension analysis of subcortical gray matter structures in schizophrenia. *PLoS One* 2016;11:e0155415.
11. Chen Y, Pham TD. Sample entropy and regularity dimension in complexity analysis of cortical surface structure in early Alzheimer's disease and aging. *J Neurosci Methods* 2013;215:210-7.
12. Pham TD, Abe T, Oka R, et al. Measures of morphological complexity of gray matter on magnetic resonance imaging for control age grouping. *Entropy* 2015;17:8130-51.
13. Riecher-Rössler A, Gschwandtner U, Aston J, et al. The Basel early-detection-of-psychosis (FePsy)-study — design and preliminary results. *Acta Psychiatr Scand* 2007;115:114-25.
14. Riecher-Rössler A, Aston J, Ventura J, et al. Das Basel Screening Instrument für Psychosen (BSIP): entwicklung, aufbau, reliabilität und validität [article in German]. *Fortschr Neurol Psychiatr* 2008;76:207-16.
15. Yung, AR, Pan Yuen, H, McGorry, PD, et al. Mapping the onset of psychosis: the comprehensive assessment of at-risk mental states. *Aust N Z J Psychiatry* 2005;39:964-71.
16. Coupe P, Yger P, Prima S, et al. An optimized blockwise nonlocal means denoising filter for 3-D magnetic resonance images. *IEEE Trans Med Imaging* 2008;27:425-41.
17. Wiest-Daesslé N, Prima S, Coupé P, et al. Rician noise removal by non-local means filtering for low signal-to-noise ratio MRI: applications to DT-MRI. *Med Image Comput Comput Assist Interv* 2008;11:171-9.
18. Rajapakse JC, Giedd JN, Rapoport JL. Statistical approach to segmentation of single-channel cerebral MR images. *IEEE Trans Med Imaging* 1997;16:176-86.
19. Manjón JV, Tohka J, García-Martí G, et al. Robust MRI brain tissue parameter estimation by multistage outlier rejection. *Magn Reson Med* 2008;59:866-73.
20. Cuadra MB, Cammoun L, Butz T, et al. Comparison and validation of tissue modelization and statistical classification methods in T1-weighted MR brain images. *IEEE Trans Med Imaging* 2005;24:1548-65.
21. Korda AI, Andreou C, Avram M, et al. Chaos analysis of the brain topology in first-episode psychosis and clinical high risk patients. *Front Psychiatry* 2022;13:965128.
22. Korda AI, Ventouras E, Asvestas P, et al. Convolutional neural network propagation on electroencephalographic scalograms for detection of schizophrenia. *Clin Neurophysiol* 2022;139:90-105.
23. Luders E, Thompson PM, Narr KL, et al. A curvature-based approach to estimate local gyrification on the cortical surface. *Neuroimage* 2006;29:1224-30.
24. Palaniyappan L, Marques TR, Taylor H, et al. Cortical folding defects as markers of poor treatment response in first-episode psychosis. *JAMA Psychiatry* 2013;70:1031-40.
25. Nelson EA, White DM, Kraguljac NV, et al. Gyrification connectomes in unmedicated patients with schizophrenia and following a short course of antipsychotic drug treatment. *Front Psychiatry* 2018;9:699.
26. Zuliani R, Delvecchio G, Bonivento C, et al. Increased gyrification in schizophrenia and non affective first episode of psychosis. *Schizophr Res* 2018;193:269-75.
27. Sasabayashi D, Takayanagi Y, Takahashi T, et al. Increased occipital gyrification and development of psychotic disorders in individuals with an at-risk mental state: a multicenter study. *Biol Psychiatry* 2017;82:737-45.
28. Das T, Borgwardt S, Hauke DJ, et al. Disorganized gyrification network properties during the transition to psychosis. *JAMA Psychiatry* 2018;75:613-22.
29. Matsuda Y, Ohi K. Cortical gyrification in schizophrenia: current perspectives. *Neuropsychiatr Dis Treat* 2018;14:1861-9.
30. Fortea A, Batalla A, Radua J, et al. Cortical gray matter reduction precedes transition to psychosis in individuals at clinical high-risk for psychosis: a voxel-based meta-analysis. *Schizophr Res* 2021;232:98-106.
31. Fusar-Poli P, Radua J, McGuire P, et al. Neuroanatomy of vulnerability to psychosis: a voxel-based meta-analysis. *Neurosci Biobehav Rev* 2011;35:1175-85.
32. Guo S, Palaniyappan L, Liddle PF, et al. Dynamic cerebral reorganization in the pathophysiology of schizophrenia: a MRI-derived cortical thickness study. *Psychol Med* 2016;46:2201-14.
33. Palaniyappan L. Progressive cortical reorganisation: a framework for investigating structural changes in schizophrenia. *Neurosci Biobehav Rev* 2017;79:1-13.
34. Im K, Lee JM, Yoon U, et al. Fractal dimension in human cortical surface: multiple regression analysis with cortical thickness, sulcal depth, and folding area. *Hum Brain Mapp* 2006;27:994-1003.
35. Yunzhi P, Chen X, Chen E, et al. Prognostic associations of cortical gyrification in minimally medicated schizophrenia in an early intervention setting. *Schizophrenia* 2022;8:88.